

Exact Solution of a Time-Varying Capacitance Problem*

J. R. MACDONALD†, FELLOW, IRE, AND D. E. EDMONDSON‡

Summary—By means of a new method, a closed-form solution is obtained for the harmonics generated by a sinusoidally varying capacitance in series with a fixed resistor and battery. The solution describes the behavior of the condenser microphone, the vibrating-reed electrometer, a vibrating plate contact potential measuring apparatus, and a special loudspeaker improvement. With only minor modifications the solution can also apply to the case of a sinusoidally varying resistance in series with a fixed inductance and battery; thus, it may, in addition, be used to calculate the response of a carbon microphone. The present large-signal solution, which applies for any finite values of the modulation index and frequency, is compared with previous small-signal approximate results, and the dependence on modulation index and frequency is investigated for such quantities as output waveform, total harmonic distortion, harmonic amplitude and phase, and average input and output power. A very distorted waveshape is obtained for low relative frequencies and values of the modulation index near and including unity.

INTRODUCTION

Few time-varying circuit problems have been solved to yield exact expressions for the harmonic components and thus, to allow their large-signal behavior to be investigated. With the current general interest in parametric amplifiers, such problems are becoming of more importance. Parametric amplifiers generally involve time-varying components, such as capacitors, in circuits which involve both inductive and capacitive energy storage. Exact large-signal analysis of such systems is very difficult and is not attempted herein. Instead, we shall be concerned only with the simpler problem of capacitive energy storage and shall show that here, at least, it is possible to give an exact solution in closed form.

Fig. 1 shows a circuit in which the center plate of a double capacitance can be moved by an outside force. We shall be concerned only with the case in which the equilibrium position of the center plate is such that $(C_1)_0 = (C_2)_0 \equiv C_0$, where the zero subscripts denote equilibrium. In addition, we shall take $R_1 = R_2 \equiv R$ and $C_3 = C_4$. In the resulting antisymmetrical push-pull circuit there is no interaction between the top and bottom circuit halves, and initial attention can therefore be restricted to the top, or single-ended, half alone. Finally, it will be assumed that the restoring force acting on the center electrode when it is displaced from

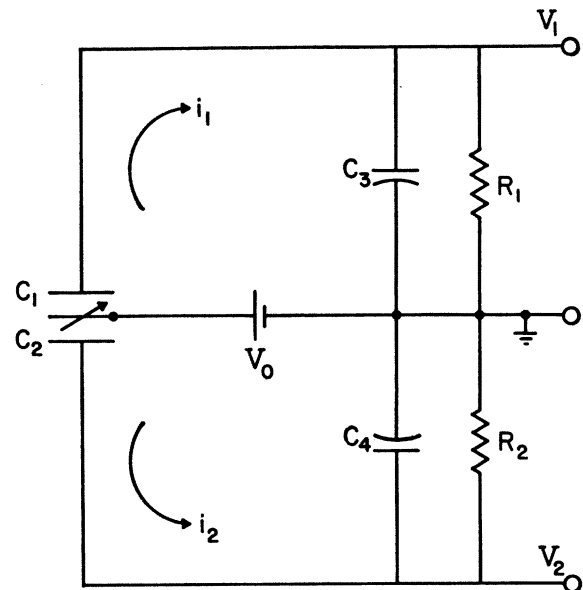


Fig. 1—Circuit diagram for time-varying double capacitor.

equilibrium is proportional to the displacement, so that the system is mechanically linear. For the present analysis we shall focus attention on the electrical part of the problem, as shown in Fig. 1, and shall not be concerned with mechanical impedances and the details of electromechanical coupling between the movable plate and the outside world.

When the movable capacitor plate is driven sinusoidally, the resulting time-varying current which flows in the circuit of Fig. 1 will not generally be sinusoidal but will contain harmonics of the driving signal. Such harmonic generation, while similar to that which arises in a nonlinear circuit, occurs here in a linear time-varying system which obeys a linear differential equation and satisfies the principle of superposition. Harmonics are produced here because of the time-varying capacitance and not principally because of the inverse dependence of capacitance on electrode spacing.

The circuit of Fig. 1 can represent a variety of devices of physical interest. First, it can be used as a representation of a single-ended or push-pull condenser microphone.¹ It can also be used to analyze the behavior

* Received by the IRE, June 2, 1960; revised manuscript received October 14, 1960.

† Texas Instruments, Inc., Dallas, Tex.

‡ Southern Methodist University, Dallas, Tex. Presently at the University of Texas, Austin.

¹ F. V. Hunt, "Electroacoustics," John Wiley & Sons, Inc., New York, N. Y., p. 170; 1954.

H. F. Olson, "Acoustical Engineering," D. Van Nostrand Co., Inc., Princeton, N. J., p. 253; 1957.

of a capacitance type of displacement probe.² In addition, it applies to the vibrating plate method of contact potential measurement^{3,4} and to the vibrating reed electrometer.⁵ As shown in Appendix VI, the present analysis, with relatively few changes, can also be used for a treatment of the carbon microphone where a time-varying resistance is in series with a time-independent inductance. Finally, the treatment applies as well to the special loudspeaker discussed below.

The magnetic loudspeaker is one of the weakest links in the high-quality reproduction of sound. Its performance has sometimes been somewhat improved by negative feedback derived from an auxiliary voice-coil winding and applied around the driving amplifier. This approach is only partially successful, especially for heavy-coned, low-frequency loudspeakers, because the voice-coil current has only partial control over cone motion and is not, therefore, a true measure of the output sound. More ideal control of cone motion can be obtained by metallizing the cone and making it the center electrode moving between two fixed metal-screen electrodes in front of and behind the cone. If bias is applied as shown in Fig. 1, the motion of the cone will generate a push-pull output signal between electrodes 1 and 2 which can be used for negative feedback. This signal will be a better measure of average cone motion and sound output than any that could be derived from the voice coil. Using it for negative feedback will result in flatter frequency response, lower nonlinear distortion, and possibly even some improvement, because of averaging, in the deleterious effects of cone breakup when it occurs. Note that the above arrangement is, in some sense, the inverse of the usual push-pull electrostatic loudspeaker where electric forces are used to move the center membrane instead of the magnetic forces of the present system. Although the same electrostatic forces exist in the present situation, they are negligible compared to the magnetic driving forces. After the above speaker improvement system was thought of by one of the present authors, a patent describing a single-ended version of the device was discovered.⁶ It will be shown later that the push-pull system without feedback can exhibit much less nonlinear distortion generation than the single-ended system.

In the present analysis of the circuit of Fig. 1, we shall be concerned with the simplest case, that of sinusoidal driving force, such as that occurring when a con-

denser microphone is exposed to a single-frequency sound source. There have not been many treatments of the present problem, and none has been carried to such a stage that it is practical to calculate the high-order harmonics which are of importance at low relative frequencies and high values of the modulation index, m . Wente⁷ analyzed the condenser microphone in 1917 and gave results valid for the fundamental response at low m and high relative frequencies only. Since then, the most ambitious treatment of the problem seems to have been that of Anderson and Alexander.⁴ They have dealt with the cases where there is no parallel fixed capacitance C_3 across R and where C_3 is nonzero, but their analysis of the latter situation is incorrect. As we shall show later, such capacitance can usually be made negligible in practice, and it will be neglected in much of the present work because it considerably complicates the analysis.

ANALYSIS

Consider the top half of Fig. 1 only, with $i_1 \equiv i$, $C_1 \equiv C$, and $R_1 \equiv R$. The basic equation to be solved is then

$$\frac{dq}{dt} = \frac{V_1}{R} + C_3 \frac{dV_1}{dt}, \quad (1)$$

where q is the instantaneous charge on C and $V_1 = V_0 - (q/C)$. Eq. (1) can be manipulated to yield

$$\frac{dq}{dt} + \frac{q}{R(C + C_3)} \left[1 - \frac{C_3 R}{C} \left(\frac{dC}{dt} \right) \right] = \left(\frac{C}{C + C_3} \right) \frac{V_0}{R}. \quad (1')$$

The quantity we wish to calculate is the steady-state value of i/i_0 , where $i_0 \equiv V_0/R$. This quantity can be written from (1') as

$$\begin{aligned} (i/i_0) = & \left(\frac{C}{C + C_3} \right) \\ & - \frac{q}{V_0(C + C_3)} \left[1 - \frac{RC_3}{C} \left(\frac{dC}{dt} \right) \right], \quad (1'') \end{aligned}$$

which can be calculated when $C(t)$ and $q(t)$ are known.

Eq. (1') may be formally integrated by means of an integrating factor when $C(t)$ is specified. The result involves rather unwieldy integrals however, and further analysis will be carried out here only for the simpler case, for which $C_3 = 0$. Then, a steady-state solution for i/i_0 is of the form

$$\begin{aligned} \left(\frac{i}{i_0} \right) = & 1 - \frac{1}{RC} \exp \left[-\frac{1}{R} \int \frac{dt}{C} \right] \\ & \cdot \int \exp \left[\frac{1}{R} \int \frac{dt}{C} \right] dt. \quad (2) \end{aligned}$$

⁷ E. C. Wente, "A condenser transmitter as a uniformly sensitive instrument for the absolute measurement of sound intensity," *Phys. Rev.*, vol. 10, pp. 39-63; July, 1917.

² R. D. Shattuck, "Capacitance-type displacement probe," *J. Acoust. Soc. Am.*, vol. 31, pp. 1297-1299; October, 1959.

³ W. A. Zisman, "A new method of measuring contact potential differences in metals," *Rev. Sci. Instr.*, vol. 3, pp. 367-370; July, 1932.

⁴ J. R. Anderson and A. E. Alexander, "Theory of the vibrating condenser converter and application to contact potential measurement," *Australian J. Appl. Sci.*, vol. 3, pp. 201-209; September, 1952.

⁵ H. Palevsky, R. K. Swank, and R. Grenchik, "Design of dynamic condenser electrometer," *Rev. Sci. Instr.*, vol. 18, pp. 298-314; May, 1947.

⁶ G. H. Brodie, U. S. Patent No. 2,857,461; October 21, 1958.

Further progress requires knowledge of the time variation of C . We shall assume that the spacing between the plane-parallel plates of C is given by $d = d_0(1 + m \sin \omega t)$ for an input driving frequency of $(\omega/2\pi)$. Here m is a modulation factor usually satisfying $0 \leq m \leq 1$. Then, neglecting fringing effects, taking rigid capacitor plates, and assuming that the driving frequency is sufficiently low that Maxwell's equations need not be invoked, one may write

$$C = C_0 / (1 + m \sin \omega t). \tag{3}$$

For simplicity, let us now introduce the new variables $\phi \equiv \omega t$, $\beta \equiv 1/RC_0$, $z \equiv \omega/\beta$, $y \equiv 1/z$, and $x \equiv my = m/z$. Also let $M \equiv (1 + m \sin \phi) \equiv C_0/C$. Note that z is a normalized frequency variable. Eq. (2) may now be simplified with the help of (3) to yield

$$\left(\frac{i}{i_0}\right) = 1 - yM e^{-y\phi + x \cos \phi} \int e^{y\phi - x \cos \phi} d\phi. \tag{4}$$

The integral in (4) cannot be carried out explicitly to yield i/i_0 in closed form. It will be shown, however, that closed expressions for the fundamental and harmonic components of i/i_0 can be obtained.

When $x \ll 1$, one can expand the exponentials involving $x \cos \phi$ in (4) in a simple power series. The integration can then be carried out and the result simplified to yield the fundamental and harmonic current components. When this procedure is applied in general, it is found that the harmonics, far from appearing in closed form, must be calculated from the product of two double series. In Appendix I, the results of this approach are given to the second order in m and up to second harmonic terms only.

Another method of handling (4) is to use the expansion⁸

$$e^{\pm x \cos \phi} = \sum_{s=0}^{\infty} \epsilon_s (\pm 1)^s I_s(x) \cos(s\phi), \tag{5}$$

where $\epsilon_0 = 1$, $\epsilon_s = 2 (s > 0)$, and $I_s(x)$ is a modified Bessel function of the first kind. When (5) is used, i/i_0 may be expressed as the product of two series or as a double series.⁹ Finally, each harmonic current component can be expressed as a single infinite series of modified Bessel functions. Such reduction is very laborious, and the resulting series are only rapidly convergent for small x . The zero-order harmonic component of i/i_0 turns out to be

$$\left(\frac{i}{i_0}\right) = 1 - \sum_{s=0}^{\infty} (-1)^s \epsilon_s I_s^2(x) \quad (0 \leq x < \infty). \tag{6}$$

⁸ W. J. Cunningham, "Introduction to Nonlinear Analysis," McGraw-Hill Book Co., Inc., New York, N. Y., p. 248; 1958.

⁹ Since the present analysis was completed, the treatment of Anderson and Alexander⁴ has been discovered. It makes use of (5), but a double series is formally avoided since the authors Fourier analyze their single-series results separately to obtain harmonic components.

Since the sum of the series may be shown to be unity, there is no static component of current, which is in agreement with the fact that a direct current cannot flow through a capacitance, even when it is varying with time as in the present case.

Another approach, and the one we shall follow in detail here, is to Fourier analyze the steady-state part of (4) directly in order to obtain closed expressions for the harmonic current components. Before Fourier analysis can be applied, the steady-state current must be expressed in terms of a definite rather than an indefinite integral. Such transformation is carried out in Appendix II with the result

$$\left(\frac{i}{i_0}\right) = 1 - \frac{yM e^{x \cos \phi}}{(e^{2\pi y} - 1)} \int_0^{2\pi} e^{y\mu - x \cos(\phi + \mu)} d\mu. \tag{7}$$

Next, we wish to express i/i_0 in the complex Fourier series

$$\left(\frac{i}{i_0}\right) = \sum_{n=-\infty}^{\infty} c_n e^{in\phi} = \frac{a_0}{2} + \sum_{s=1}^{\infty} \{a_s \cos s\phi + b_s \sin s\phi\}, \tag{8}$$

where $c_n \equiv (a_n - ib_n)/2$.

The complicated calculation of the complex coefficients c_n is carried out in Appendix III. The final closed-form results are

$$c_0 = 0, \tag{9}$$

$$c_n = \frac{in\pi}{\sinh \pi y} I_{iy}(x) \cdot I_{n-iy}(x). \quad (n > 0). \tag{10}$$

Eq. (10) is difficult to use directly for numerical calculations because of the imaginary and complex orders of the modified Bessel functions appearing in it. As shown in Appendix IV, however, recursion relations may be established between the complex and real harmonic coefficients of different orders. These relations allow the coefficients for any harmonic order to be calculated provided those for the two adjacent orders are known. One simple way of obtaining such initial starting coefficients is to calculate them directly from the power series expansion of (10). The necessary results are developed in Appendix V. Once a_1 , a_2 , b_1 , and b_2 are calculated, the recursion relations of Appendix IV allow coefficients of higher orders to be obtained quite simply. Although the calculation of the initial a 's and b 's requires series evaluation, the series are far simpler than those obtained by the other methods of solution discussed briefly above, and the convergence of the present series is such that they are useful for much higher x values than could be treated practically by other methods.

The quantity $z = y^{-1} = RC_0\omega$ is a normalized frequency variable proportional to the ratio of the time constant of the undisturbed system to the period of the driving force. In addition, the following symbols will be used in

the next section. Each harmonic component of i/i_0 appears in the form

$$h_n(\phi) \equiv a_n \cos n\phi + b_n \sin n\phi \tag{11}$$

$$= \alpha_n \sin(n\phi + \chi_n),$$

where

$$\alpha_n \equiv (a_n^2 + b_n^2)^{1/2}, \tag{12}$$

and

$$\chi_n \equiv \sin^{-1}(a_n/\alpha_n). \tag{13}$$

In addition to the harmonic amplitude α_n , we shall also be interested in the normalized amplitude $\gamma_n \equiv (\alpha_n/\alpha_1)$. The total harmonic distortion (THD) given by

$$\text{THD} \equiv \left[\sum_{r=2}^{\infty} \alpha_r^2 \right]^{1/2} / \left[\sum_{r=1}^{\infty} \alpha_r^2 \right]^{1/2} \tag{14}$$

is likewise a quantity of interest. When the entire circuit of Fig. 1 is operated in the push-pull mode with $C_1=C_2$ and $R_1=R_2$, the symmetry of the arrangement is such that no even-order harmonics appear between the 1-2 terminals. In this case, it is pertinent to define the modified total harmonic distortion factor (MTHD) by

$$\text{MTHD} \equiv \left[\sum_{r=2}^{\infty} \alpha_{2r-1}^2 \right]^{1/2} / \left[\sum_{r=1}^{\infty} \alpha_{2r-1}^2 \right]^{1/2}, \tag{15}$$

an expression which involves odd harmonics only.

Using an IBM 650 digital computer, (49)–(52), and (59) in Appendixes V and VI have been summed for values of z and m that are of interest. In such summation, additional terms of the series are calculated until a term is reached which is sufficiently small to cause no change, within the eight-figure precision of the computer, in the partial sum to that point. This procedure, which yields sums of maximum computer accuracy, is necessary because the recursion relations (42) and (43) require starting values as correct as possible to allow accurate higher order harmonic components to be calculated.

DISCUSSION OF RESULTS

Since the series for the harmonic components are convergent for any finite value of x , they can be used for very large x values, which can correspond to high values of m and low values of z , the normalized frequency. Although $m=1$ is not usually a useful value for the physical devices discussed in the Introduction, it is found that there is a smooth transition from $m=0.99$ to $m=1$, and it is therefore convenient to consider this limiting case. The pertinent series converge, in fact, for $m > 1$; so the limitation $m < 1$, when pertinent, is physical, not mathematical. It would be possible to use an analog computer to represent the circuit of Fig. 1 in such a way that negative capacitances were realized. In

this case, m could exceed unity, and the present mathematical results would still apply. However, since the physical devices which the mathematical results describe are limited to $m < 1$ or $m \leq 1$, the numerical calculations leading to the results of the present section have been also limited to the range $0 < m \leq 1$.

Fig. 2 shows how the distortion factors depend on frequency for various values of m . It will be noted that for $z \ll 1$ both THD and MTHD approach limiting values which, in the case of THD, are very nearly equal to m . Thus, for example, no matter how low the frequency, the maximum total harmonic distortion for $m=0.01$ is one per cent. For $z \gg 1$, both THD and MTHD decrease as the frequency increases with limiting slopes of -1 and -2 , respectively. As expected, MTHD is always less than THD even at very low frequencies.

Fig. 3 presents the distortion factors as a function of m with z the parameter. These graphs show clearly that only for high values of m near unity can decreasing z below 0.1 make any very appreciable difference in THD and MTHD. Such decrease, however, can change the harmonic constitution considerably. The limiting slopes in Fig. 3(a) are unity, while those in 3(b) are equal to two. The dotted lines show the linear extrapolations of the curves.

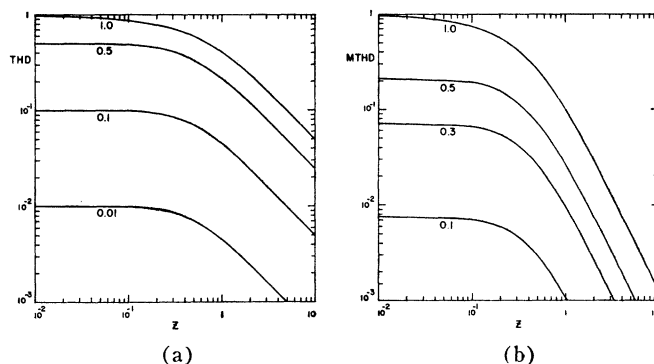


Fig. 2—Harmonic distortion factors, THD and MTHD, as functions of normalized frequency z for various values of the modulation index m .

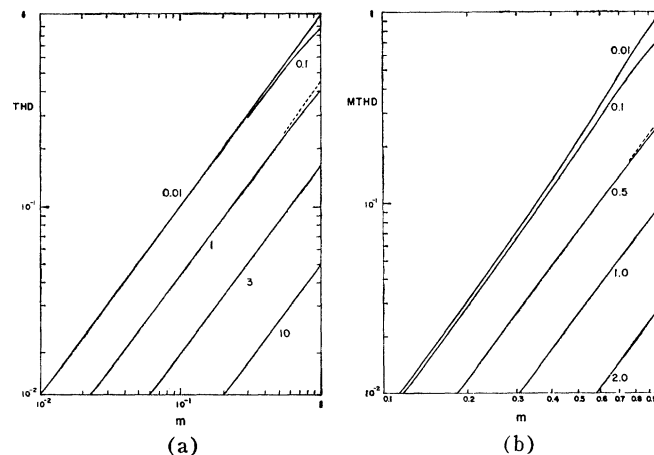


Fig. 3—THD and MTHD vs m for various values of z .

For most of the practical devices to which the present analysis applies, it is desirable to operate under conditions which minimize harmonic distortion. Fig. 4 is drawn for THD and MTHD values of one per cent and shows how m and z must be interrelated to maintain these values. To the right of each curve the distortion will be less than one per cent. Clearly, for a given z , m may be much higher for a total push-pull harmonic distortion of one per cent than for a single-ended total harmonic distortion of the same value. The limiting slopes in this figure are both two.

Another quantity like THD or MTHD which is determined by the entire spectrum of harmonics is the rms relative wave amplitude. We shall actually plot the amplitude

$$A = \left(\sum_{n=1}^{\infty} \alpha_n^2 \right)^{1/2}$$

which is $\sqrt{2}$ times the rms amplitude. The quantity A reduces to the zero-to-peak amplitude of the wave only when a single sinusoidal component is present. Thus, for large z , it approaches α_1 which, in turn, approaches m . For push-pull operation we shall take A as

$$\left(\sum_{r=1}^2 \alpha_{2r-1}^2 \right)^{1/2}$$

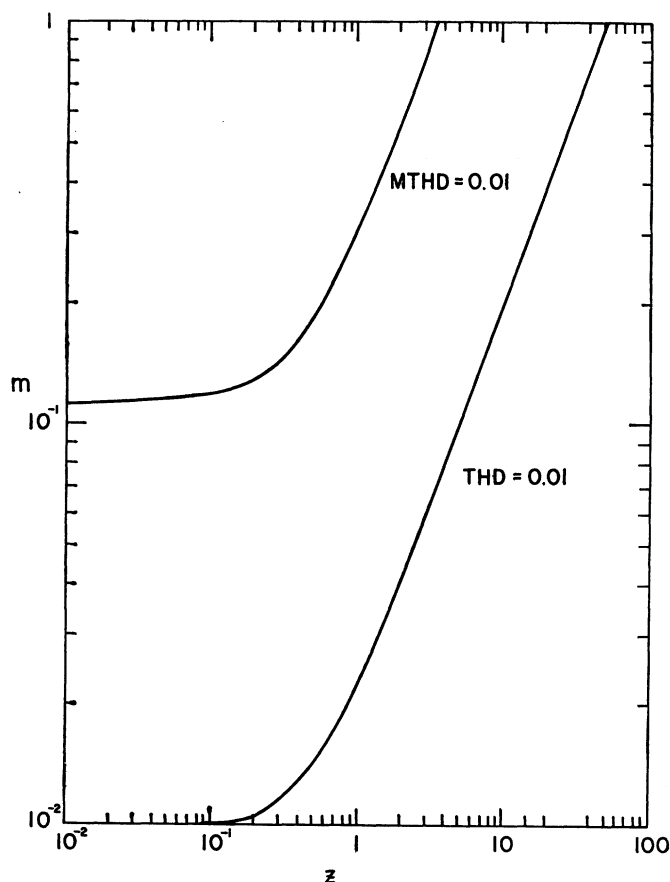


Fig. 4—Interrelation between m and z necessary for MTHD and THD to remain constant and equal to 0.01.

for convenient comparison with that for single-ended operation. Fig. 5 shows how A depends on z for $m=0.5$ and 1. The limiting slopes for the $m=0.5$ curves are unity, the usual 6 db/octave slope to be expected for a capacitive reactance. Note that when the single-ended and push-pull curves are very close together, only the fundamental is of importance.

The equations for all the above quantities which depend on sums of harmonics have been written with an infinite upper limit. In practice, as the harmonic index n increases, one eventually reaches a region where higher harmonic amplitudes are decreasing so rapidly that further harmonics add nothing appreciable to the series. In the machine calculations, summation of the series are always carried to this point even when n values as high as 25 are required.

Fig. 6 shows how the normalized harmonic amplitudes depend on the order of the harmonic for various m and z values. We have connected the calculated

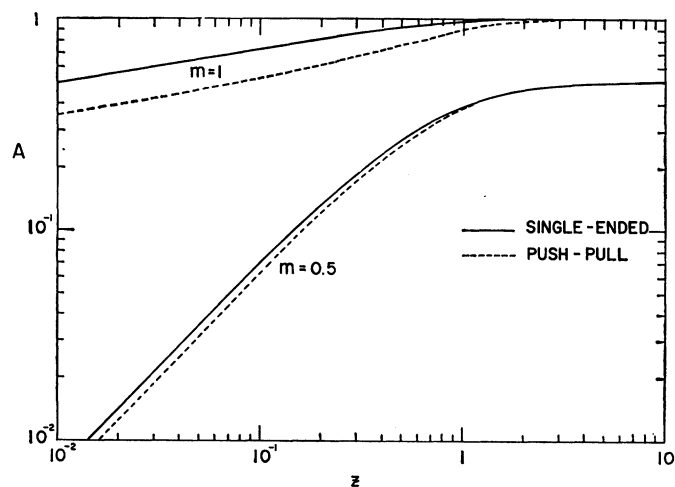


Fig. 5—Dependence on normalized frequency of the single-ended and push-pull amplitudes, A , for $m=0.5$ and 1.

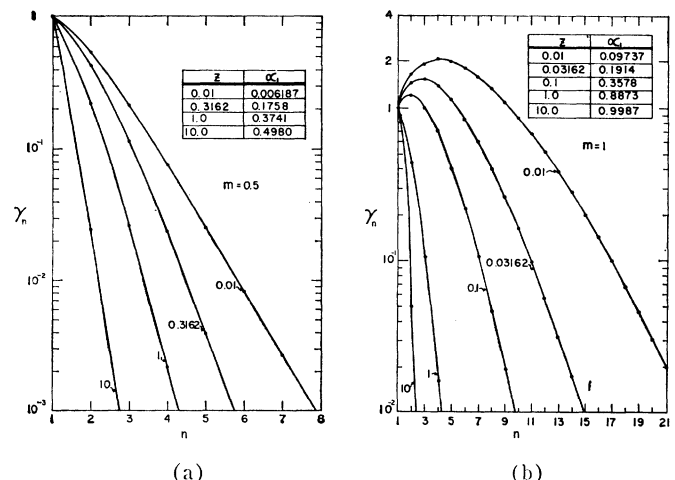


Fig. 6—Dependence of normalized harmonic amplitudes, $\gamma_n = \alpha_n/\alpha_1$, on harmonic index, n , for $m=0.5$ and 1 and various z values.

points with light lines for convenience, but only the dots themselves are significant. Also shown in the tables are the fundamental amplitude values, α_1 , for the various z values considered. For $z \gg 1$, α_1 approaches m . As expected, the harmonic amplitudes decrease very rapidly when z is unity or greater. When $z = 1$, $\omega RC_0 = 1$; so $z = 1$ is a natural dividing point. When $z \gg 1$, the period of the driving force is much smaller than the natural time constant RC_0 . Under these conditions, the charge on the variable capacitance cannot change appreciably within a period, and the instantaneous voltage across the capacitor will be proportional to $1/C$ and will thus involve the fundamental component only. In the limit of high frequencies, the variable capacitor charge q will remain virtually constant and there will be no harmonic generation.

For $n \geq 3$, the harmonics in Fig. 6 have been calculated using the recursion relations of Appendix IV. These relations eventually involve small differences between large numbers and, as n increases, harmonic coefficient accuracy will eventually become impaired. With the eight significant figures available on the 650 machine, this point is reached when γ_n has decreased somewhat below 0.01. The value of γ_n which is still accurate is still more than sufficiently small so that the sums involving α_n^2 converge excellently.

Anderson and Alexander⁴ have been able to apply their technique for solving the present problem to m values as high as 0.667 and to z values as small as 0.222 ($x = 3$). In this case, they obtained γ_n values of 63, 26, 9, and 1 per cent for $n = 2, 3, 4, 5$, respectively.¹⁰ For the same input, the present analysis yields 63.3, 26.7, 8.8, 2.4, and 0.58 per cent for n from 2 to 6. This is relatively good agreement and affords a check of both methods of solution.

An interesting feature of Fig. 6(b) is the rise of some of the higher harmonic amplitudes above the amplitude of the fundamental. This behavior occurs to a smaller degree as well for m values of 0.9 but has disappeared by $m = 0.7$. Curves for $m = 1$ and z , considerably less than 0.01, could not be obtained with the present 650 calculation program because it was limited to a maximum of 100 terms in each of the series of Appendixes V and VI. Some idea of how many terms in these series were required is given by the following data: for $m = 1$, the following z values: 10, 1, 0.3162, 0.1, 0.03162, and 0.01 required a maximum of 3, 7, 11, 21, 40, and 82 terms, respectively; smaller values of m of course needed fewer terms.

The harmonic coefficients a_n and b_n can be recombined when known to yield the Fourier series of (8) which allows i/i_0 to be plotted as a function of ϕ . The

resulting waveshapes for various values of z are shown in Fig. 7 (next page) for $m = 0.5$ and in Fig. 8 for $m = 1$. We have actually plotted $(1/m)(i/i_0)$ rather than (i/i_0) in order to facilitate comparison between the two figures. The $(1/m)$ factor causes the fundamental signal components to have the same amplitude at high frequencies (eg., $z \geq 10$) independently of the value of m . Also shown in these figures are dotted curves of (C/C_0) or $(C/10C_0)$ which indicate how the normalized capacitance varies through a cycle.

Fig. 7 shows that at high relative frequencies the current is in phase with the capacitance, and, even at $z = 10$, there is little distortion of the waveshape and very small phase shift. The situation is considerably changed as z decreases, however, and the harmonic components shown in Fig. 6 begin to play an important role. Note that the decrease in amplitude shown in Fig. 5 has been partly compensated in the curves for $z = 0.1$ and 0.01 by multiplying the amplitudes by the factors shown. As z decreases, the most striking alteration is that the current changes from having a maximum at $\phi = 3\pi/2$, the point where the capacitance is maximum, to going through zero at this point. In the low-frequency limit, the current curve thus tends to be proportional to the derivative of the capacitance.

Somewhat similar results are shown in Fig. 8. For $m = 1$, however, Fig. 5 shows that there is not a very appreciable decrease in the rms current amplitude as z decreases; thus, none of the curve amplitudes has been changed here. For $m = 1$, the capacitance reaches infinity at $\phi = 3\pi/2$. The equations show, however, that at this point there is no voltage across the capacitor and no charge on it. Hence, it is merely a short circuit and, at this value of ϕ , the current is limited only by the series resistance and must therefore be equal to i_0 . This requirement is independent of the value of z . As mentioned in Appendix VII, the force between the capacitor plates never becomes infinite even for $m = 1$. Except at very low relative frequencies, the force with $m = 1$ will not, in fact, vary much over a cycle. The stiffness of the suspension of the moveable plate need only be great enough to balance the static electrical attractive force and give the desired spacing, d_0 , when $V_1 = 0$ and V_0 is equal to the applied value. Note that near $\phi = 3\pi/2$ the capacitance somewhat approximates a delta function and the current approximates a doublet impulse function, the derivative of the delta function. Because of the requirement that $i = i_0$ at $\phi = 3\pi/2$, the doublet cannot be equal to zero at $\phi = 3\pi/2$, as in the $m = 0.5$ case, except in the low-frequency limit. The short-circuit condition and the resulting waveshape near $\phi = 3\pi/2$ are responsible for the slow decrease of the rms amplitude of i/i_0 for $m = 1$ as compared to that for $m = 0.5$. Note that Fourier analysis shows that the average value of (C/C_0) is $(1 - m^2)^{-1/2}$. For $m = 1$, this quantity reaches infinity, unlike the average value of a delta function which is finite. Little need be said about

¹⁰ It should be noted that Anderson and Alexander have denoted by fundamental, first harmonic, second harmonic, etc. quantities which are usually (and in the present treatment) termed fundamental or first harmonic ($n = 1$), second harmonic ($n = 2$), etc.

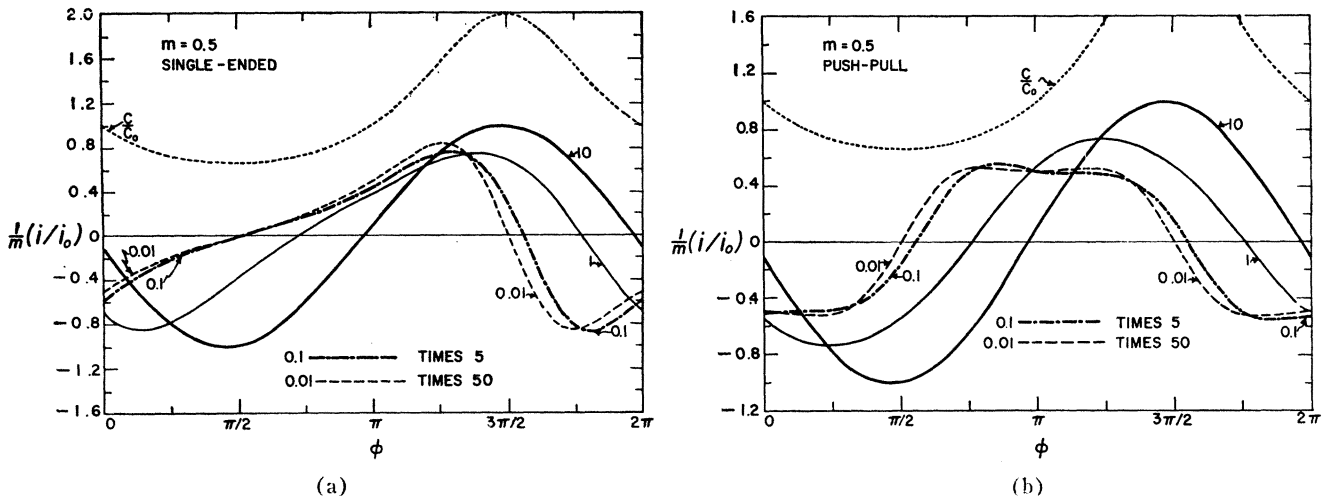


Fig. 7—Dependence of $(1/m)(i/i_0)$ on $\phi = \omega t$ for $m=0.5$ and various z values. The dotted curve shows (C/C_0) vs ϕ .

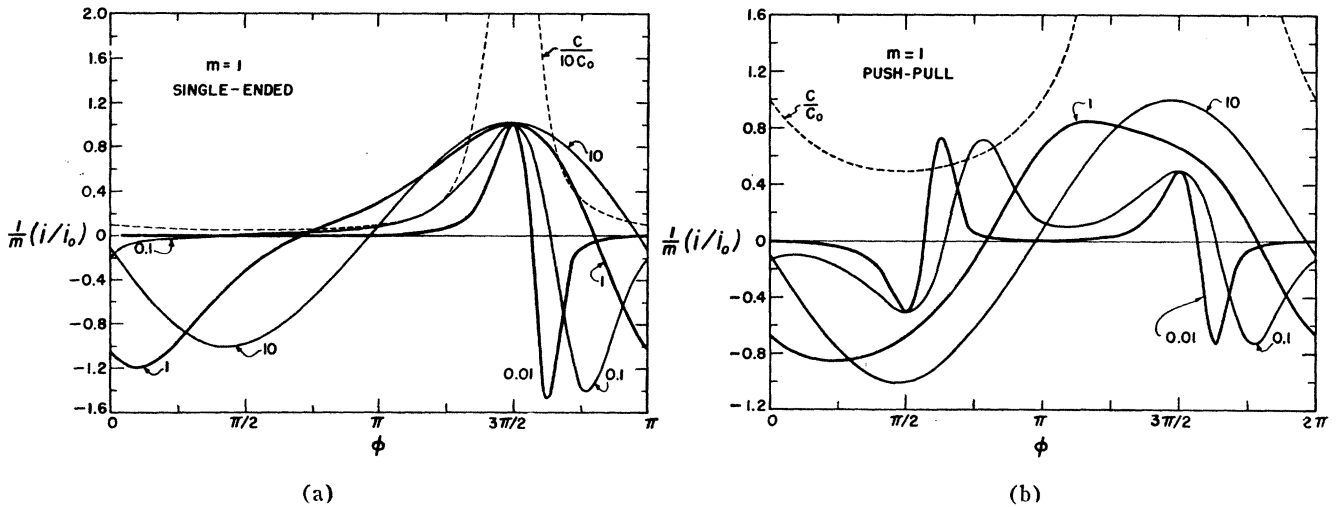


Fig. 8—Dependence of $(1/m)(i/i_0)$ on ϕ for $m=1$ and various z values. The dotted curve shows $(C/10C_0)$ in (a) and (C/C_0) in (b).

the push-pull curves; their symmetry arises from the absence of all even-order harmonics.

The question of how well the simplest approximate expressions for the harmonic coefficients given in Appendix I represent the actual behavior of the system is of some interest. For $z=0.01$ and 1 , Figs. 9 and 10 show how the ratio of exact to approximate coefficients, (α_n/α_n^0) , depends on z for $n=1, 2, 3$. For the $z=0.01$ case, the simple solution is only a good approximation for $m < 0.3$. Also, for $z=0.01$ the higher the harmonic order the worse the approximation, while for $z=1$ the reverse is true.

The results of Appendix I may also be used to compare approximate and exact phase predictions. In Fig. 11, the quantity $-\Delta\chi_n = \chi_n^0 - \chi_n$ is plotted vs m for $n=1$ and 2 and three z values. In Fig. 12, the phase results are plotted vs z in different forms. In these graphs, solid lines denote positive and dotted lines negative quantities and, for convenience in plotting, all χ_n values have been diminished by 180° . First, the accurate values of χ_1 and χ_2 in degrees are plotted. In addition, the percentage deviation of the accurate values from

the approximate values are shown. Note that very high deviations occur for χ_2 when $m=1$. The open breaks in the $(100\Delta\chi_2/\chi_2^0)$ curves near $z=0.6$ appear because in this region the signs of the approximate and accurate second harmonic phases are different.

Finally, Fig. 13 (page 461) shows how the zero frequency or dc harmonic amplitude in the carbon microphone case (Appendix VI) depends on modulation for various frequency values. One sees that in this case, where a dc component is allowed, the dc part of i can greatly exceed $i_0 = V_0/R_0$ when m is near unity and z is small. This is an interesting case of rectification without nonlinearity.

For low harmonic distortion yet appreciable m , z must be unity or greater. It is of interest to inquire what value of R is necessary to ensure that $z=1$ at $f=20$ cps in the modified loudspeaker discussed in the Introduction. Since the capacitance modification will be of most value for large, low-frequency speakers, we may consider a typical cone area of 1300 cm^2 . If the fixed screens are 0.25 inch in front of and behind the cone, the single-ended equilibrium capacitance is about 181

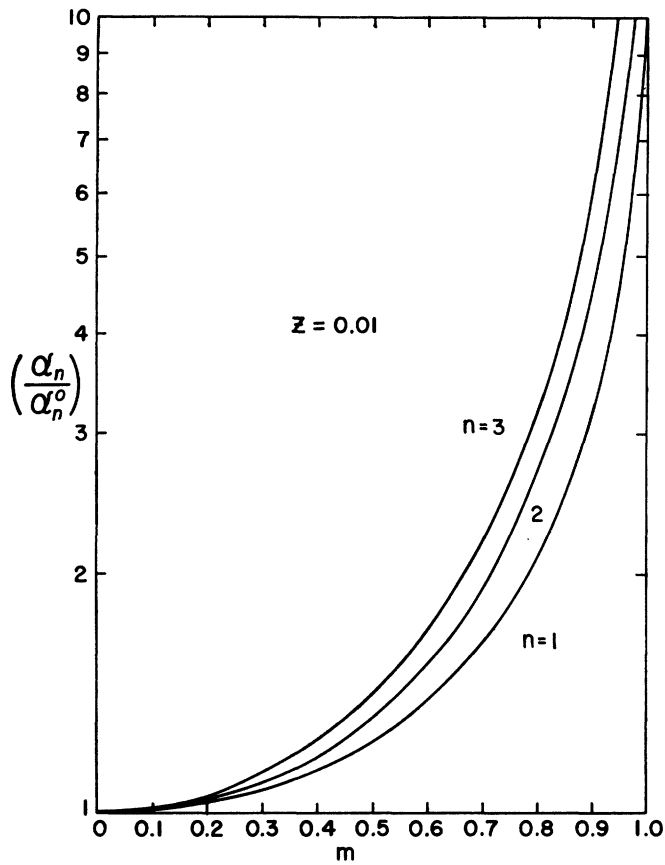


Fig. 9—Comparison of exact and approximate harmonic amplitudes as functions of m for $z=0.01$.

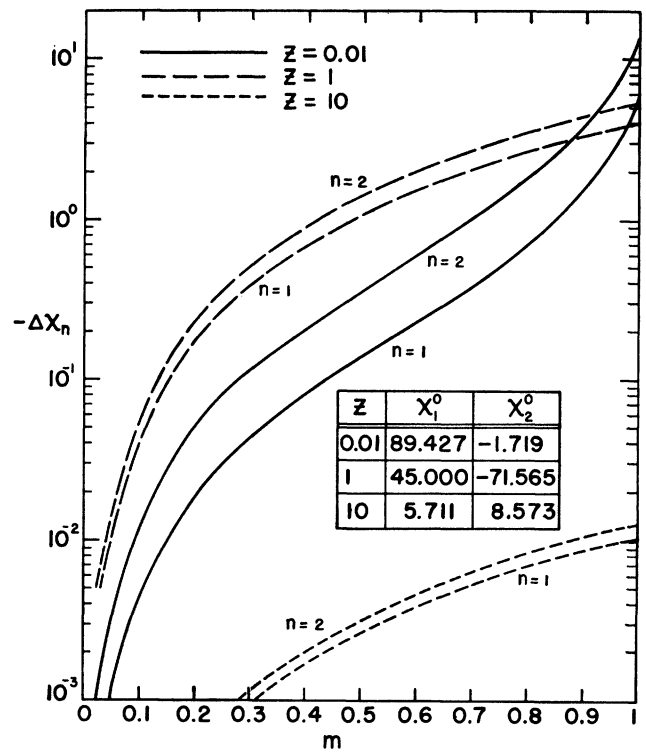


Fig. 11—Dependence of phase difference $-\Delta X_n = X_n^0 - \chi_n$ on m for $n=1$ and 2 and various z values.

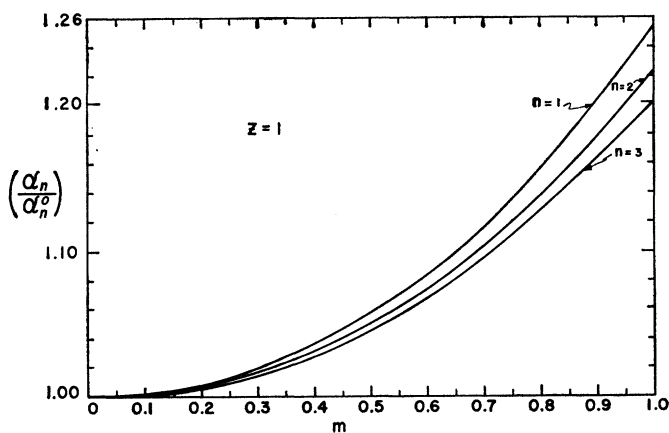


Fig. 10—Comparison of exact and approximate harmonic amplitudes as functions of m for $z=1$.

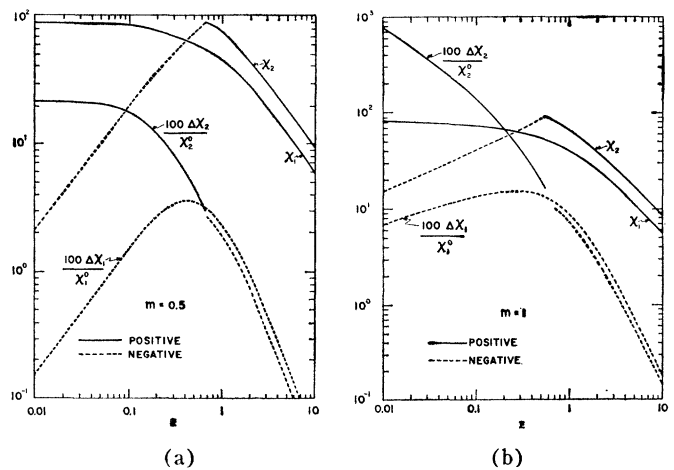


Fig. 12—Dependence of χ_1 and χ_2 in degrees on z for $m=0.5$ and 1 , and dependence on z of percentage differences between accurate and approximate phases.

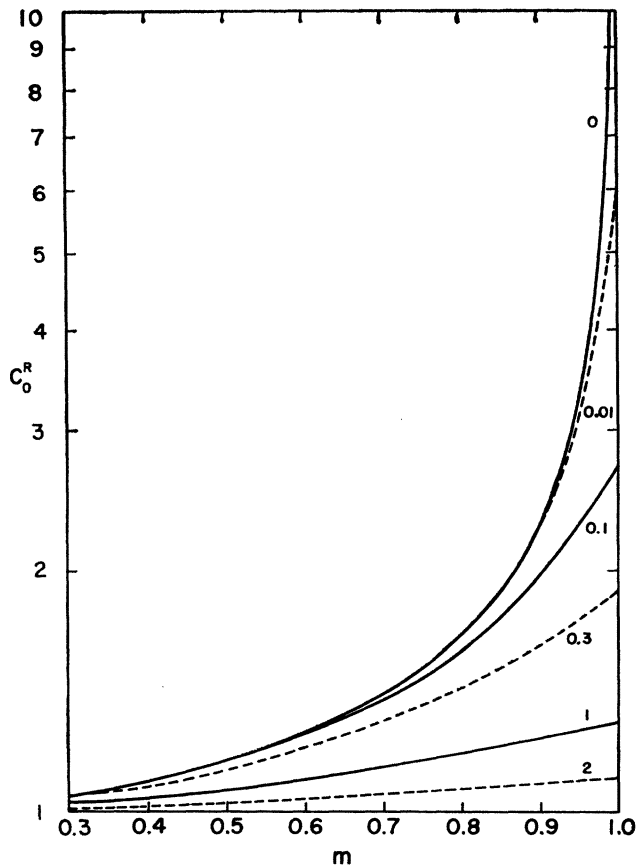


Fig. 13—Dependence of dc component of (i/i_0) in the carbon microphone case on m for several z values.

p.f. This leads to an R value of 44 megohms, an easily realized magnitude. Note that the present analysis applies only when R is much less than the leakage resistance of C . It was mentioned earlier that the capacitance C_3 in parallel with R would be neglected. Exact conditions which must be met by C_3 to justify such neglect have not been derived. It is clear, however, that one necessary condition is that $C_3 \ll C_0$ for any m . Further, if the load is to remain primarily resistive, it is essential for all frequencies of interest that the reactance of C_3 appreciably exceed the magnitude of R . If we require a capacitive reactance of 100 megohms at $f=1000$ cps, the parallel capacitance must be less than 0.016 p.f. This is a reasonably stringent requirement, but it can be met by fairly well-known feedback techniques^{11,12} which make it possible to achieve an amplifier input impedance made up of a resistive component exceeding 10^9 ohms and virtually zero input capacitance over the audio frequency range.

In Appendix VII, expressions are derived for the instantaneous values of the vibrating capacitor charge, voltage, stored energy, power dissipated in the vibrating capacitor, attraction between plates, input power,

and the power developed in the load resistor, R . In addition, a general relation, (69), between the instantaneous powers in the system is established. The behavior of the capacitor voltage, V_c , can be obtained directly from the results already presented for (i/i_0) . The other quantities involve functions of the integral F_1 (Appendix II) which has not been evaluated in closed form. It is of interest, therefore, to calculate the time averages of these quantities where possible.

The average power output, equal to the average power input, is obtained in Appendix VII in a series form valid for arbitrary frequency. Averages of the other quantities may also be obtained as infinite series, but only the first few terms, applicable for $z \gg 1$, are calculated in the Appendix. It will be noted from (71) that the average output power, $\langle P_{out} \rangle$, equals $A^2 V_0^2 / 2R$ where A is the ordinate of Fig. 5 and has been defined earlier. For $z \gg 1$, $\langle P_{out} \rangle$ approaches $m^2 V_0^2 / 2R$. For $z=0.01$ and $m=1$, the results of Fig. 5 show that $\langle P_{out} \rangle \simeq V_0^2 / 8R$, indicating that the output power has not dropped off tremendously even at this low z value. The input power calculated in Appendix VII is the ideal minimum and involves only the power required to move the charged plates of the capacitor against the electrical forces involved. In practice, there will be unavoidable electromechanical conversion losses, but such power dissipation can often be made small.

The rich harmonic generation shown in Fig. 6(b) suggests that a vibrating capacitor device could be used for efficient high harmonic production. However, the conversion efficiency is lowered by the efficiency of whatever electromechanical, piezoelectric, electrostrictive, or magnetostrictive device is used to vibrate one of the capacitor plates, and the resulting over-all efficiency may not be comparable to that obtained with all-electric harmonic converters. When a voltage-dependent capacitance^{13,14} is used in place of the mechanically driven capacitor, the nonlinearity of this device may possibly contribute even greater high harmonic generation if C_{min}/C_{max} can be made sufficiently small.

It is often desired to obtain high harmonics from a frequency-stabilized quartz crystal since the resulting harmonics will themselves be well frequency stabilized. The vibrating capacitor may possibly be useful here. Consider a quartz crystal vibrating in a longitudinal mode. One end of it is metallized and may be considered the vibrating plate of a capacitor. The quartz crystal is attached to a rigid rectangular C-shaped structure in such a way that the top of it vibrates very close to the top of the C , which can be the fixed plate of the capacitor. By forming this fixed capacitance of aluminum with a thin anodized insulating surface, values of m at

¹¹ J. R. Macdonald, "An ac cathode follower circuit of very high input impedance," *Rev. Sci. Instr.*, vol. 25, pp. 144-147; February, 1954.

¹² J. R. Macdonald, "Some augmented cathode follower circuits," *IRE TRANS. ON AUDIO*, vol. AU-5, pp. 63-70; May-June, 1947.

¹³ D. B. Leeson and S. Weinreb, "Frequency multiplication with nonlinear capacitors—a circuit analysis," *PROC. IRE*, vol. 47, pp. 2076-2084; December, 1959.

¹⁴ L. J. Giacoletto and J. O'Connell, "A variable-capacitance germanium junction diode for UHF," *RCA Rev.*, vol. 17, pp. 68-85; March, 1956.

least as large as 0.95 should be achievable and operation with $m=1$ should also be possible on elimination of this layer. Operation with $z=0.01$ or below will then lead to the generation of harmonics of high order and accurately controlled frequency.

APPENDIX I

POWER SERIES EXPANSION

To second order in m ($x=my$), we may write

$$e^{\pm x \cos \phi} = 1 \pm x \cos \phi + (x^2 \cos^2 \phi)/2. \quad (14)$$

The quantity i/i_0 may be expressed in general as the Fourier series given in (8) of the body of this work. Substituting (14) in (4), simplifying, and comparing with (8) yields

$$\left. \begin{aligned} a_0 &= 0 \\ a_1 &= -mz/(1+z^2) \\ a_2 &= \frac{-3m^2z^2}{(1+z^2)[1+(2z)^2]} \\ b_1 &= -mz^2/(1+z^2) \\ b_2 &= -\frac{m^2z(2z^2-1)}{(1+z^2)[1+(2z)^2]} \end{aligned} \right\}. \quad (15)$$

The harmonic amplitudes $\alpha_n \equiv \sqrt{a_n^2 + b_n^2}$ are, for $n=1, 2, 3$,

$$\left. \begin{aligned} \alpha_1^0 &= mz/\sqrt{1+z^2} \\ \alpha_2^0 &= m\alpha_1^0/\sqrt{1+(2z)^2} \\ \alpha_3^0 &= 3m\alpha_2^0/4\sqrt{1+(3z)^2} \end{aligned} \right\}, \quad (16)$$

where the zero superscript indicates that the quantities in question are of lowest order in m . Note that as $z \rightarrow \infty$, $i/i_0 \rightarrow -m \sin \phi$, the correct result in this limit.

APPENDIX II

TRANSFORMATION OF (4)

Let

$$i/i_0 \equiv 1 - yMF_1, \quad (17)$$

where

$$\begin{aligned} F_1(\phi) &\equiv e^{-y\phi+x \cos \phi} \int e^{y\phi-x \cos \phi} d\phi \\ &= e^{-y\phi+x \cos \phi} \left[c + \int_0^\phi e^{y\lambda-x \cos \lambda} d\lambda \right]. \end{aligned} \quad (18)$$

In the last equation, c is an integration constant. Next, we wish to find the steady-state or periodic part of $F_1(\phi)$. We have

$$\begin{aligned} F_1(\phi + 2\pi k) &= e^{-2\pi yk} \left\{ e^{-y\phi+x \cos \phi} \left[c + \int_0^\phi e^{y\lambda-x \cos \lambda} d\lambda \right] \right. \\ &\quad \left. + e^{-y\phi+x \cos \phi} \int_\phi^{\phi+2\pi k} e^{y\lambda-x \cos \lambda} d\lambda \right\} \end{aligned}$$

$$\begin{aligned} &= e^{-2\pi yk} \left[F_1(\phi) + e^{-y\phi+x \cos \phi} \sum_{s=0}^{k-1} \int_{\phi+2\pi s}^{\phi+2\pi(s+1)} e^{y\lambda-x \cos \lambda} d\lambda \right] \\ &= e^{-2\pi yk} [F_1(\phi) + F_2(\phi)], \end{aligned} \quad (19)$$

where k is a positive integer.

On making the transformation $\mu \equiv \lambda - \phi - 2\pi s$, the last integral becomes

$$\begin{aligned} &\int_0^{2\pi} e^{y(\mu+\phi+2\pi s)-x \cos(\mu+\phi+2\pi s)} d\mu \\ &= e^{y\phi+2\pi sy} \int_0^{2\pi} e^{y\mu-x \cos(\mu+\phi)} d\mu. \end{aligned}$$

Thus,

$$\begin{aligned} F_2(\phi) &= e^x \cos \phi \sum_{s=0}^{k-1} e^{2\pi sy} \int_0^{2\pi} e^{y\mu-x \cos(\mu+\phi)} d\mu \\ &= e^x \cos \phi \int_0^{2\pi} e^{y\mu-x \cos(\mu+\phi)} d\mu \cdot \sum_{s=0}^{k-1} e^{2\pi sy} \\ &= \left(\frac{e^{2\pi ky} - 1}{e^{2\pi y} - 1} \right) e^x \cos \phi \int_0^{2\pi} e^{y\mu-x \cos(\mu+\phi)} d\mu \end{aligned} \quad (y \neq 0). \quad (20)$$

Substituting (20) into (19) with $a \equiv (e^{2\pi y} - 1)^{-1}$ yields

$$\begin{aligned} F_1(\phi + 2\pi k) &= e^{-2\pi yk} \left[F_1(\phi) - a e^x \cos \phi \int_0^{2\pi} e^{y\mu-x \cos(\mu+\phi)} d\mu \right] \\ &\quad + a e^x \cos \phi \int_0^{2\pi} e^{y\mu-x \cos(\mu+\phi)} d\mu. \end{aligned} \quad (19')$$

If the last term is denoted $F_3(\phi)$, we have

$$F_1(\phi + 2\pi k) = e^{-2\pi yk} [F_1(\phi) - F_3(\phi)] + F_3(\phi). \quad (19'')$$

Since $F_3(\phi + 2\pi k) = F_3(\phi)$, we may write

$$F_1(\phi + 2\pi k) - F_3(\phi + 2\pi k) = e^{-2\pi yk} [F_1(\phi) - F_3(\phi)]. \quad (21)$$

Now since $[F_1(\phi) - F_3(\phi)]$ is bounded for $0 \leq \phi \leq 2\pi$ and $y > 0$, (21) shows that F_1 approaches F_3 uniformly in ϕ for large ϕ . Thus, for large t ($\phi \rightarrow \infty$)

$$F_1(\phi) \rightarrow F_3(\phi) = a e^x \cos \phi \int_0^{2\pi} e^{y\mu-x \cos(\mu+\phi)} d\mu. \quad (22)$$

Applying (22) in (17) yields (7) of the text.

APPENDIX III

FOURIER ANALYSIS

Using the notation and results of Appendix II, the complex Fourier coefficients are given by

$$\begin{aligned} c_n &= \frac{1}{2\pi} \int_0^{2\pi} [1 - yMF_3] e^{-in\phi} d\phi \\ &= \frac{1}{2\pi} \int_0^{2\pi} e^{-in\phi} d\phi - \frac{1}{2\pi} \int_0^{2\pi} yMF_3 e^{-in\phi} d\phi. \end{aligned} \quad (23)$$

Thus, with

$$\frac{1}{2\pi} \int_0^{2\pi} e^{-in\phi} d\phi \equiv \delta_{0n} = 1 \quad (n = 0) \quad \text{and} \quad 0 \quad (n > 0),$$

we may write

$$\begin{aligned} &(\delta_{0n} - c_n) \\ &= \frac{a}{2\pi} \int_0^{2\pi} (y + x \sin \phi) e^{-in\phi+x \cos \phi} \int_0^{2\pi} e^{y\mu-x \cos(\phi+\mu)} d\mu d\phi \\ &= \frac{a}{2\pi} \int_0^{2\pi} (y + x \sin \phi) e^{-in\phi-y\phi+x \cos \phi} \\ &\quad \cdot \int_0^{2\pi} e^{y(\phi+\mu)-x \cos(\phi+\mu)} d\mu d\phi. \end{aligned} \tag{24}$$

Now let,

$$G(\phi) \equiv \int_0^{2\pi} e^{y(\phi+\mu)-x \cos(\phi+\mu)} d\mu, \tag{25}$$

and

$$g(\phi) \equiv e^{-(y+in)\phi+x \cos \phi}. \tag{26}$$

Integrating (24) by parts yields

$$\begin{aligned} (\delta_{0n} - c_n) &= \frac{a}{2\pi} \left\{ [-g(\phi)G(\phi)]_0^{2\pi} + \int_0^{2\pi} g(\phi) \frac{dG}{d\phi} d\phi \right. \\ &\quad \left. - in \int_0^{2\pi} g(\phi)G(\phi) d\phi \right\}, \end{aligned} \tag{27}$$

where

$$\begin{aligned} \frac{dG}{d\phi} &= \frac{d}{d\phi} \int_{\phi}^{2\pi+\phi} e^{y\lambda-x \cos \lambda} d\lambda = [e^{y(\phi+2\pi)-x \cos \phi} - e^{y\phi-x \cos \phi}] \\ &= e^{y\phi-x \cos \phi} [e^{2\pi y} - 1]. \end{aligned} \tag{28}$$

The first term in (27) is zero and substituting (28) in (27) leads to

$$(\delta_{0n} - c_n) = \frac{1}{2\pi} \int_0^{2\pi} e^{-in\phi} d\phi - \frac{ina}{2\pi} \int_0^{2\pi} g(\phi)G(\phi) d\phi. \tag{29}$$

Thus, $c_0 = 0$ and for $n > 0$, one obtains

$$\begin{aligned} c_n &= \frac{ina}{2\pi} \int_0^{2\pi} g(\phi)G(\phi) d\phi \\ &= \frac{ina}{2\pi} \int_0^{2\pi} \int_0^{2\pi} e^{y\mu-in\phi+2x \sin \mu/2 \sin(\phi+\mu/2)} d\mu d\phi \\ &= \frac{ina}{2\pi} \int_0^{2\pi} e^{y\mu+in\mu/2} d\mu \int_0^{2\pi} e^{-in(\phi+\mu/2)+2x \sin \mu/2 \sin(\phi+\mu/2)} d\phi \\ &= \frac{ina}{2\pi} \int_0^{2\pi} e^{y\mu+in\mu/2} d\mu \int_{\mu/2}^{\mu/2+2\pi} e^{-in\xi+2x \sin \mu/2 \sin \xi} d\xi. \end{aligned} \tag{30}$$

Since the second integral is periodic, we may write

$$\begin{aligned} c_n &= \frac{ina}{2\pi} \int_0^{2\pi} e^{y\mu+in\mu/2} d\mu \int_0^{2\pi} e^{-i[n\xi+2ix \sin \mu/2 \sin \xi]} d\xi, \\ &= \frac{ina}{2\pi} \int_0^{2\pi} e^{y\mu+in\mu/2} J_n(-2ix \sin \frac{\mu}{2}) d\mu. \end{aligned} \tag{31}$$

On making the substitution $\mu/2 \equiv \pi/2 + \theta$,

$$c_n = 2inae^{y\pi} \int_{-\pi/2}^{\pi/2} e^{2y\theta+in\theta} e^{in\pi/2} J_n(-2ix \cos \theta) d\theta. \tag{32}$$

Since

$$I_n(x) = e^{-in\pi/2} J_n(xe^{in\pi/2}), \tag{33}$$

and

$$J_n(xe^{-i\pi}) = e^{-in\pi} J_n(x), \tag{34}$$

we may write

$$\begin{aligned} e^{in\pi/2} J_n(-2ix \cos \theta) &= e^{in\pi/2} e^{-in\pi} J_n(2ix \cos \theta) \\ &= e^{-in\pi/2} J_n(2ix \cos \theta) = I_n(2x \cos \theta). \end{aligned} \tag{35}$$

Thus,

$$c_n = 2inae^{y\pi} \int_{-\pi/2}^{\pi/2} e^{(2y+in)\theta} I_n(2x \cos \theta) d\theta. \tag{36}$$

This result can finally be further simplified as follows:

$$\begin{aligned} c_n &= 2inae^{y\pi} \int_0^{\pi/2} [e^{(2y+in)\theta} + e^{-(2y+in)\theta}] I_n(2x \cos \theta) d\theta \\ &= \frac{2in}{\sinh \pi y} \int_0^{\pi/2} \cos [(n - 2iy)\theta] I_n(2x \cos \theta) d\theta \\ &= \frac{2in}{\sinh \pi y} \int_0^{\pi/2} \cos \{ [(n - iy) - iy]\theta \} \\ &\quad I_{(n-iy)+iy}(2x \cos \theta) d\theta. \end{aligned} \tag{37}$$

Now, we may make use of the identity¹⁵

$$I_\mu(x)I_\nu(x) = \frac{2}{\pi} \int_0^{\pi/2} I_{\mu+\nu}(2x \cos \theta) \cos \{(\mu - \nu)\theta\} d\theta \tag{38}$$

to obtain the final result

$$c_n = \frac{in\pi}{\sinh \pi y} I_{iy}(x)I_{n-iy}(x). \quad (n > 0). \tag{39}$$

APPENDIX IV

RECURSION RELATIONS

Using a recursion relation satisfied by $I_\nu(x)$, (10) may be written as ($n \geq 1$), hence

$$c_n = \frac{i\pi n x}{2(n - iy) \sinh \pi y} I_{iy}(x) \cdot [I_{n-1-iy}(x) - I_{n+1-iy}(x)]. \tag{40}$$

¹⁵ G. N. Watson, "A Treatise On the Theory of Bessel Functions" Cambridge University Press, Cambridge, Eng.; 1944. See p. 150 for the equation expressed in terms of ordinary Bessel functions.

This result may be expressed in the form

$$c_n = \frac{nx}{2(n-iy)} \left[\frac{c_{n-1}}{n-1} - \frac{c_{n+1}}{n+1} \right], \quad (40')$$

a recursion relation between the complex harmonic coefficients. Next we require similar relations between the real coefficients a_n and b_n . From (40') we have

$$(a_{n+1} - ib_{n+1}) = \left(\frac{n+1}{n-1} \right) (a_{n-1} - ib_{n-1}) - \frac{2(n+1)}{nx} (n-iy) [a_n - ib_n], \quad (41)$$

which leads to the final results

$$a_{n+1} = \left(\frac{n+1}{n-1} \right) a_{n-1} - \frac{2(n+1)}{nx} (na_n - yb_n), \quad (42)$$

$$b_{n+1} = \left(\frac{n+1}{n-1} \right) b_{n-1} - \frac{2(n+1)}{nx} (nb_n + ya_n). \quad (43)$$

APPENDIX V
SERIES EXPANSIONS

Eq. (10) may be written in the form

$$c_n = \frac{in\pi}{\sinh \pi y} H(x), \quad (n > 0). \quad (44)$$

The last result must be simplified. We have

$$\Gamma(n-iy+s+1) = \prod_{r=1}^n (s+r-iy) \cdot \Gamma(s+1-iy), \quad (46)$$

$$\begin{aligned} &\Gamma(s+1-iy)\Gamma(s+1+iy) \\ &= \Gamma(iy)\Gamma(-iy) \prod_{r=0}^s [(r+iy)(r-iy)] \\ &= \frac{\pi}{y} \operatorname{csch} \pi y \prod_{r=0}^s (r^2 + y^2). \end{aligned} \quad (47)$$

Thus,

$$c_n = iny \sum_{s=0}^{\infty} \frac{\left(\frac{x}{2}\right)^{n+2s} (n+2s)! \prod_{r=1}^n (s+r+iy)}{s!(n+s)! \prod_{r=0}^s (r^2 + y^2) \cdot \prod_{r=1}^n [(s+r)^2 + y^2]}. \quad (48)$$

When c_n is set equal to $(a_n - ib_n)/2$, series for the real coefficients can be obtained. Because of the complex product in the numerator of (48), such separation becomes progressively more complicated as n increases. Hence, it is convenient that series results need only be obtained for $n=1$ and 2 , with the recursion relations used for higher n . Separation yields the series

$$a_1 = -2y^2 \sum_{s=0}^{\infty} \frac{(x/2)^{1+2s} (1+2s)!}{s!(1+s)! [(1+s)^2 + y^2] \prod_{r=0}^s (r^2 + y^2)}, \quad (49)$$

$$b_1 = -2y \sum_{s=0}^{\infty} \frac{(x/2)^{1+2s} (1+2s)!}{[s!]^2 [(1+s)^2 + y^2] \prod_{r=0}^s (r^2 + y^2)}, \quad (50)$$

$$a_2 = -4y^2 \sum_{s=0}^{\infty} \frac{(x/2)^{2+2s} (2+2s)! (3+2s)}{s!(2+s)! [(1+s)^2 + y^2] [(2+s)^2 + y^2] \prod_{r=0}^s (r^2 + y^2)}, \quad (51)$$

$$b_2 = -4y \sum_{s=0}^{\infty} \frac{(x/2)^{2+2s} (2+2s)! [(1+s)(2+s) - y^2]}{s!(2+s)! [(1+s)^2 + y^2] [(2+s)^2 + y^2] \prod_{r=0}^s (r^2 + y^2)}, \quad (52)$$

where

$$\begin{aligned} H(x) &\equiv I_{n-iy}(x) I_{iy}(x) \\ &= e^{-in\pi/2} J_{n-iy}(ix) J_{iy}(ix) \\ &= (i)^{-n} J_{n-iy}(ix) J_{iy}(ix) \\ &= \sum_{s=0}^{\infty} \frac{(x/2)^{n+2s} \Gamma(n+2s+1)}{s! \Gamma(n+s+1) \Gamma(n-iy+s+1) \Gamma(iy+s+1)}, \end{aligned} \quad (45)$$

and the last result follows from a Bessel function expansion given by Watson.¹⁶

¹⁶ *Ibid.*, p. 147.

These series are absolutely convergent for $0 \leq x \leq \infty$. It is worth pointing out that their initial terms ($s=0$) agree with the results of Appendix I when $z=y^{-1}$ is used.

For numerical summation of the above series, it is worth pointing out that they all involve simple functions of s times the quantity

$$A_s \equiv \frac{(2s)!}{2^{2s} s!} = \frac{1}{2^{2s}} \binom{2s}{s}, \quad (53)$$

and A_s satisfies the recursion relation $A_{s+1} = [(s+\frac{1}{2})/(s+1)] A_s (s > 0)$ and $A_0 = 1$.

APPENDIX VI
CARBON MICROPHONE

Consider a single-ended carbon microphone in series with a battery, V_0 , and an inductance L , the primary of an input transformer. If a sinusoidal sound wave of frequency $(\omega/2\pi)$ impinges on the microphone, its resistance R will be given by $R=R_0(1+m \sin \omega t)$, where the modulation factor $m(0 \leq m \leq 1)$ depends on the amplitude of the incident wave. The pertinent differential equation for the current i is

$$\frac{di}{dt} + \left(\frac{R_0}{L}\right)(1 + m \sin \omega t) = \frac{V_0}{L} \tag{54}$$

A steady-state solution is of the form,

$$\left(\frac{i}{i_0}\right) = ye^{-y\phi+x \cos \phi} \int e^{y\phi-x \cos \phi} d\phi, \tag{55}$$

which should be compared with (4). Here $i_0 \equiv V_0/R_0$ as before, but $y = (\omega L/R_0)^{-1}$ since the time constant is now $\tau_0 \equiv L/R_0$ rather than RC_0 as in the capacitance problem.

Because of the similarity of (55) and (4), it is readily shown that the steady-state current is given by

$$\left(\frac{i}{i_0}\right) = \frac{ye^{x \cos \phi}}{(e^{2\pi y} - 1)} \int_0^{2\pi} e^{y\mu-x \cos(\phi+\mu)} d\mu, \tag{56}$$

and

$$c_n = \frac{\pi y}{\sinh \pi y} I_{iy}(x) \cdot I_{n-iy}(x), \quad (n \geq 0). \tag{57}$$

a result only slightly different from (10). Note particularly, however, that c_0 is no longer zero, and there is thus a zero-frequency component in the current. In particular, we have (using an R superscript for the present case)

$$c_0^R = \frac{2y}{\sinh \pi y} \int_0^{\pi/2} \cosh(2\theta y) I_0(2x \cos \theta) d\theta, \tag{58}$$

$$= y^2 \sum_{s=0}^{\infty} \binom{2s}{s} \frac{(x/2)^{2s}}{\prod_{r=0}^s (r^2 + y^2)}. \tag{59}$$

Note that $c_0^R \rightarrow 1$ as $m \rightarrow 0$ and also as $\omega \rightarrow \infty$. As ω approaches zero, however, the sum of the series for c_0^R approaches a limit greater than unity for $m > 0$. In this case the series may be summed and yields $c_0^R = (1 - m^2)^{-1/2}$. The excess over unity arises from rectification of some of the incident energy by time-varying resistance of the microphone. Clearly, infinite incident energy is necessary to cause $m = 1$ in the limit of zero frequency. For $n > 0$ we have

$$c_n^R = (y/in)c_n^C, \quad (n > 0). \tag{60}$$

where the R and C superscripts denote the carbon microphone and capacitance values, respectively, of the

complex Fourier coefficients. It immediately follows that

$$\alpha_n^R = (y/n)\alpha_n^C \tag{61}$$

$$\chi_n^R = \chi_n^C - 90^\circ. \tag{62}$$

A push-pull, or double-button, carbon microphone can be handled in the same general way as the push-pull capacitance microphone.

APPENDIX VII
POWER RELATIONS

Let $\xi \equiv (i/i_0)$. It is readily shown that

$$\left. \begin{aligned} q &= CV_0(1 - \xi) \\ &= C_0V_0(1 - \xi)/M \equiv q_0(1 - \xi)/M, \\ V_c &= V_0(1 - \xi), \end{aligned} \right\} \tag{63}$$

where V_c is the instantaneous voltage across the time-varying capacitance C . Denote the stored energy in the capacitance by E and the work done in moving its plate by W . The instantaneous power dissipated in the capacitor will be $P_c = dE/dt$, and the instantaneous input power will be $P_{in} = dW/dt$. The force between the plates, F_c , may be written in the form $F_c = C_0V_0^2(q/q_0)^2/2d_0$. Finally, define P_{out} as the power dissipated in the output resistance, and P_0 as $\equiv V_0^2/R$.

We may immediately write

$$\begin{aligned} E &= \frac{1}{2} CV_c^2 = \frac{1}{2} C_0V_0^2(1 - \xi)^2/M \\ &\equiv E_0(1 - \xi)^2/M, \end{aligned} \tag{64}$$

$$\begin{aligned} P_c &= \frac{1}{2} V_c^2 \frac{dC}{dt} + CV_c \frac{dV_c}{dt} \\ &= iV_c - \frac{1}{2} V_c^2 \frac{dC}{dt} \\ &= P_0 \left\{ (1 - \xi) \left[\xi - \frac{1}{2} (1 - \xi) R \frac{dC}{dt} \right] \right\} \\ &= P_0 \left\{ (1 - \xi) \left[\xi + \frac{mz \cos \phi}{2M^2} (1 - \xi) \right] \right\}, \end{aligned} \tag{65}$$

where

$$i = V_c \frac{dC}{dt} + C \frac{dV_c}{dt}$$

has been used. Since

$$dW = F_c dd = F_c d_0 m \omega \cos \phi dt,$$

P_{in} becomes

$$\begin{aligned} P_{in} &= F_c d_0 m \omega \cos \phi \\ &= P_0 [m \omega R C_0 \cos \phi (q/q_0)^2/2], \end{aligned} \tag{66}$$

and P_{out} is

$$P_{out} = P_0 \xi^2. \tag{67}$$

Now, using $\xi = 1 - yMF_1$, where F_1 is the integral defined in Appendix II, the desired quantities may be written as

$$\left. \begin{aligned} q/q_0 &= yF_1, \\ V_c/V_0 &= MyF_1, \\ E/E_0 &= M(yF_1)^2, \\ P_c/P_0 &= (MyF_1) - (MyF_1)^2 + \frac{mz \cos \phi}{2} (yF_1)^2, \\ F_c/F_0 &= (yF_1)^2, \\ P_{in}/P_0 &= \frac{mz \cos \phi}{2} (yF_1)^2, \\ P_{out}/P_0 &= 1 - 2(MyF_1) + (MyF_1)^2, \end{aligned} \right\} \quad (68)$$

where $F_0 \equiv C_0 V_0^2 / 2d_0$. Note that the expression for F_c shows that this force will not become infinite even when $m = 1$. The above equations lead to the general relationship,

$$(P_{in}/P_0) + (i/i_0) = (P_c/P_0) + (P_{out}/P_0). \quad (69)$$

Next, it is desirable to obtain the average values of the above quantities in the steady state. For this purpose, the quantity F_1 must be replaced by F_3 . It has already been shown in Appendix III that for the steady state $c_0 = 0$; thus $\langle \xi \rangle = 0$ and $\langle MyF_3 \rangle = 1$, where the pointed brackets denote time averages. This absence of a dc current means that the battery cannot supply power on the average to the load resistance. Some of the above averages are difficult to carry out because of the presence of the integral F_3 in them, but the next two results avoid such difficulties. We have,

$$\begin{aligned} \langle P_c/P_0 \rangle &= \frac{1}{2\pi} \int_0^{2\pi} \frac{dE}{dt} d\phi \\ &= \frac{\omega}{2\pi} [E(2\pi) - E(0)] = 0, \end{aligned} \quad (70)$$

where the last equation follows from the stationary, periodic character of the stored capacitor energy. Then,

Parseval's theorem may be applied to yield the following expression for $\langle P_{out}/P_0 \rangle$, valid for $0 \leq x < \infty$,

$$\begin{aligned} \langle P_{out}/P_0 \rangle &= \langle \xi^2 \rangle = -1 + \langle (MyF_3)^2 \rangle \\ &= 2 \sum_{n=1}^{\infty} |c_n|^2, \end{aligned} \quad (71)$$

noting that $c_0 = 0$. We may now write,

$$\left. \begin{aligned} \langle q/q_0 \rangle &= \langle yF_3 \rangle, \\ \langle V_c/V_0 \rangle &= \langle MyF_3 \rangle = 1, \\ \langle E/E_0 \rangle &= \langle M(yF_3)^2 \rangle, \\ \langle P_c/P_0 \rangle &= 1 - \langle (MyF_3)^2 \rangle + \frac{mz}{2} \langle (yF_3)^2 \cos \phi \rangle \\ &= 0, \\ \langle F_c/F_0 \rangle &= \langle (yF_3)^2 \rangle, \\ \langle P_{in}/P_0 \rangle &= \frac{mz}{2} \langle (yF_3)^2 \cos \phi \rangle. \end{aligned} \right\} \quad (72)$$

Note that (69) leads to $\langle P_{in} \rangle = \langle P_{out} \rangle$, a necessary condition since the battery can supply no average power.

Although it has not been found practical to evaluate the remaining averages in (72) in closed form, it is possible to use (14) and expand F_3 in a series useful for $x \ll 1$ and $z \gg 1$. Using the resulting series, the necessary averaging may be carried out, and one finds for high relative frequencies the following terms to second order in x ,

$$\left. \begin{aligned} \langle q/q_0 \rangle &= 1 + (x^2/2) + \dots, \\ \langle E/E_0 \rangle &= 1 + (x^2/2) + \dots, \\ \langle F_c/F_0 \rangle &= 1 + (3x^2/2) + \dots, \\ \langle P_{in}/P_0 \rangle &= \langle P_{out}/P_0 \rangle \\ &= (m^2/2) - (1 - m^2)(x^2/2) + \dots \end{aligned} \right\} \quad (73)$$

ACKNOWLEDGMENT

The authors are grateful to P. Carnahan and G. Milner for their work in programming the present problem for the IBM computer. Helpful comments from G. K. Walters and T. L. Estle are also appreciated.